A 1D simplified approach for liquefaction potential evaluation of soil deposits

Gabriele Boccieri[1], Domenico Gaudio[2][0000-0001-8957-5764] and Riccardo Conti[1][0000-0001-7255-4537]

[1] Università Niccolò Cusano, Rome, Italy
[2] Sapienza Università di Roma, Rome, Italy
gabriele.boccieri@unicusano.it

Abstract. Build-up of seismic-induced pore water pressures in saturated sandy soils and the resulting reduction of effective stresses may lead to dramatic consequences. Indeed, as observed during several seismic events occurred over the last decade (Tohoku, Japan and Christchurch, New Zealand 2011; Emilia, Italy 2012; Palu, Indonesia 2018), severe damage due to liquefaction has caused both economic and environment-wise adverse impacts. Therefore, the development of a reliable although simplified tool for the assessment of liquefaction risk may be favorably perceived both in the Academia and in the current practice.
In this framework, the paper presents an improvement of the uncoupled method originally proposed by Seed *et al.* [1], where the excess pore water pressures induced by seismic loading under partially-drained conditions were evaluated. In their work, the Authors modified the well-known Terzaghi one-dimensional consolidation equation by adding a source term, which represents the rate of excess pore pressures generated under fully-undrained conditions. The governing equation is hereby solved using the Finite Difference Method implemented in a homemade *Matlab* script, taking into account the drainage conditions related to soil layering and possible filtering of the input motion caused by soil stiffness degradation, which in turn is induced by the excess pore pressure build-up. The proposed implementation is validated against the results of fully-coupled 1D FE analyses carried out with the Finite Element code *Plaxis* 2D, where the response of liquefiable sandy layers is reproduced through the advanced constitutive model SANISAND [2].

Keywords: Liquefaction, Simplified Approach, Numerical Analyses.

1 Introduction

As recognized from post-earthquake surveys (Niigata, Japan 1964; Christchurch, New Zealand 2011; Palu, Indonesia 2018), liquefaction phenomena, which are triggered by seismic-induced excess pore water pressures in saturated sandy soils, may result in catastrophic consequences. This topic was addressed by several researchers over the last decades, who aimed at providing reliable tools for the design practice. Among these,

rigorous numerical methods, which make use of advanced constitutive models to reproduce the nonlinear soil behaviour, are typically too onerous, difficult to calibrate and time-consuming. As a result, the liquefaction potential of a given soil deposit is usually assessed using a *decoupled* approach, where the seismic loading is computed through a total-stress Site Response Analysis (SRA), while the earthquake-induced excess pore water pressures are estimated based on semi-empirical relationships.

Starting from the work by Seed *et al.* [1], Boccieri *et al*. [3] developed a *Matlab* [4] routine, which implements the *decoupled* approach using the Finite Difference Method (FDM). This paper introduces two relevant modifications with respect to [3]: (i) the influence of excess pore water pressures on the signal propagation through the soil column is taken into account in a simplified fashion; (ii) a more realistic hypothesis is introduced for the time distribution of equivalent cycles, overcoming the assumption of uniform distribution adopted in the original work.

The new approach is validated against fully-coupled Finite Element (FE) analyses, carried out with *Plaxis* 2D [5], where the mechanical behaviour of the liquefiable sand is simulated through the advanced constitutive model SANISAND [2].

2 Decoupled approach

The proposed method is based on the *decoupled* approach outlined by Seed *et al*. [1], which basically can be split in two stages: (1) a total-stress 1D SRA to compute accelerations and shear stresses along the soil column; and (2) a consolidation analysis to evaluate the seismic-induced excess pore water pressures, u, within the soil deposit. Regarding the second phase, they added a source term to the classical 1D consolidation equation [6], which then reads:

$$\frac{\partial u}{\partial t} = c_v \frac{\partial^2 u}{\partial z^2} + \frac{\partial u_g}{\partial t} \tag{1}$$

where c_v is the consolidation coefficient, and $\partial u_g/\partial t$ represents the rate of the excess pore pressure build-up under fully-undrained conditions, which can be computed based on the results of cyclic undrained tests.

The *decoupled* approach underlying the method allows to compute the pore water pressure build-up in partially-drained conditions via Eq. (1), after assessing the seismic-induced shear stresses through a preliminary total-stress 1D SRA. The source term is linked to the irregular shear stress time history, which in turn is converted to an equivalent cyclic loading with constant amplitude, $\tau_{eq} = 0.65\ \tau_{max}$ (where τ_{max} is the maximum shear stress), equivalent number of cycles N_{eq}, and duration T_d. Hence, the generative term can be rewritten as:

$$\frac{\partial u_g}{\partial t} = \frac{\sigma'_{v0}}{N_L} \cdot \frac{dr_u}{dr_N} \cdot \frac{dN}{dt} \tag{2}$$

where $r_u = u_g/\sigma'_{v0}$ is the pore pressure ratio; $r_N = N/N_L$ is the cyclic ratio; N is the n-th cycle of the loading; and N_L is the number of cycles needed to trigger liquefaction.

Regarding the dissipative term in Eq. (1), $c_v \cdot \partial^2 u/\partial z^2$, the degradation of c_v due to the excess pore water pressures induced by the seismic event was included in the model using a standard empirical equation for sands, in the form [7]:

$$G_0 = F(e)\cdot(p')^{0.5} \tag{3}$$

where G_0 is the small-strain shear stiffness, $F(e)$ is a function of the void ratio, e, and p' is the current mean effective stress, which depends on the actual value of the pore water pressure.

The assumptions introduced for the definition of the curve r_u-r_N, and for the evaluation of N_L and N_{eq}, are discussed in the following, together with an indication for the calibration of the model parameters.

2.1 Excess pore water pressures relationship and cyclic resistance curve

The r_u-r_N function provides information on the development of excess pore water pressures during an undrained cyclic loading. In this study, a power function was considered:

$$r_u = \chi\cdot(r_N)^{\theta} \tag{4}$$

where χ and θ are two curve-fitting parameters to be determined from cyclic laboratory tests. The functional form of Eq. (4) was chosen because not only it provides a good fit to the experimental data, but it is also easy to differentiate.

At a given depth within the liquefiable sand layer, the number of cycles needed to trigger liquefaction, N_L, can be obtained from a standard laboratory cyclic resistance curve CSR-N_L, where $CSR = \tau_{eq}/\sigma'_{v0}$ is the cyclic stress ratio, σ'_{v0} is the geostatic vertical effective stress and τ_{eq} is related to the maximum shear stress, τ_{max}, induced by the seismic event. The following equation was considered in this work to fit a given CSR-N_L set of experimental data:

$$CSR = CSR_t + \beta\cdot N_L^{-\eta} \tag{5}$$

where CSR_t is the threshold below which no liquefaction occurs when the soil sample is loaded cyclically in undrained conditions.

2.2 Equivalent cyclic loading

As mentioned, the irregular shear stress time history induced by the earthquake at a given depth is converted to an equivalent cyclic loading, defined by a constant amplitude τ_{eq}, a number of equivalent cycles N_{eq}, and duration T_d. Following [8], N_{eq} can be evaluated considering the CSR-N_L curve as the locus of same damage level (*i.e.* initial liquefaction), as

$$N_{eq} = \sum_{i=0}^{T_{end}} N_i\cdot X_i \qquad X_i = \begin{cases} \left(\dfrac{|CSR_{0.65}| - CSR_t}{|CSR_i| - CSR_t}\right)^{-1/\eta} & \text{if} \quad |CSR_i| > CSR_t \\ 0 & \text{if} \quad |CSR_i| \le CSR_t \end{cases} \tag{6}$$

where $CSR_{0.65} = \tau_{eq}/\sigma'_{v0}$, $CSR_i = \tau_i/\sigma'_{v0}$, while N_i and T_{end} are the number of cycles with amplitude τ_i and the duration of the input signal, respectively. The equivalent number of cycles was computed through the peak-counting method [8].

Seed *et al.* [1] considered a uniform distribution of the number of cycles over the loading duration T_d, where T_d is the strong motion duration of the input signal. Although

simple, this assumption is not representative of the effective energy content distribution over the signal duration. Therefore, the cumulative number of cycles $N(t_k)$ up to the time $t = t_k$ was considered in this work, defined as:

$$N(t_k) = \sum_{i=0}^{k} N_i \cdot X_i \tag{7}$$

Consistently, the derivative *dN/dt* is no longer constant in Eq. (2).

With the aim of computing Eq. (6) and Eq. (7), the irregular shear stress loading at a given depth was obtained by equilibrium from the SRA acceleration time histories, assuming an in-phase acceleration of the 1D soil column.

2.3 Influence of excess pore water pressures on the frequency content of the earthquake-induced soil accelerations

Soil stiffness degradation due to pore water pressures build-up can modify the frequency content of seismic waves propagating through a saturated sand layer. This was taken into account with an iterative procedure which was implemented in this work to low-pass filter the SRA accelerations consistently with the computed excess pore water pressures. An equivalent natural frequency f_{0eq} of the soil column was introduced, defined as:

$$f_{0\,eq} = \frac{V_{s\,eq}}{4 \cdot H} \tag{8}$$

where H is the total height of the 1D soil column and V_{seq} is the equivalent shear wave velocity. The latter was computed at the time instant t_{95}, corresponding to which $N(t) = 0.95 \cdot N_{eq}$ in the middle of the soil column, as:

$$V_{s\,eq} = \frac{H}{\sum_{i=1}^{n} \frac{h_i}{V_{si}}} \tag{9}$$

where h_i and $V_{si} = (G_i(p')/\rho_i)^{0.5}$ are the thickness and shear wave velocity of the i^{th} sub-layer, respectively, and $n = H/h_i$. Based on a preliminary study, a filter frequency $f_{cut} = 3 \cdot f_{0eq}$ was defined. Within the iterative procedure, the value of f_{cut} computed at the j^{th} step is used to low-pass filter the SRA accelerations used to calculate the excess pore water pressures at the $(j+1)^{th}$ step.

3 Comparison with coupled FEM analyses

The proposed FDM *decoupled* approach was validated against the results of *coupled* dynamic FE analyses, carried out with the software *Plaxis* 2D CE v20 [5]. Fig. 1a-b shows the 1D soil column considered in the analyses with the profiles of initial shear waves velocity V_{s0} and consolidation coefficient c_{v0}. The soil column is comprised of two layers: the bottom one is a liquefiable sand layer, whereas the top one was modelled as a non-liquefiable layer, consisting of either a gravelly, or a sandy or a clayey crust. The mechanical properties of the soil layers are listed in Table 1, while Fig. 1c-d shows

the acceleration time history and Fourier Amplitude spectra of the input signal, corresponding to the Northridge (1994) earthquake, low-pass filtered at 10 Hz.

The mechanical behaviour of the deepest liquefiable layer was reproduced with the SANISAND constitutive model, assuming the parameters reported for Toyoura sand [2], while the *Hardening Soil model with Small-Strain stiffness* (*HSSmall* [9]) was adopted for the top layer. Table 2 reports the relevant parameters for the *HSSmall* model, calibrated based on available literature data.

Table 1. Soil layer mechanical properties. γ_{sat} = saturated soil weight; I_p = plasticity index; e_{min} and e_{max} = minimum and maximum void ratios, respectively; e = void ratio; K_0 = at rest earth pressure coefficient ; c' = cohesion; ϕ' = friction angle; k = hydraulic conductivity

Soil	γ_{sat} (kN/m^3)	I_p (%)	e_{min} (-)	e_{max} (-)	e (-)	OCR (-)	K_0 (-)	c' (kPa)	ϕ' (°)	k (m/s)
clay	20	50	-	-	-	1	0.609	0	23.00	$1 \cdot 10^{-6}$
sand	20	-	0.597	0.977	0.650	-	0.500	0	30.00	$5 \cdot 10^{-4}$
gravel	20	-	0.435	0.923	0.740	-	0.500	0	30.00	$1 \cdot 10^{-2}$
liquef. sand	19	-	0.597	0.977	0.825	-	0.483	0	31.15	$5 \cdot 10^{-4}$

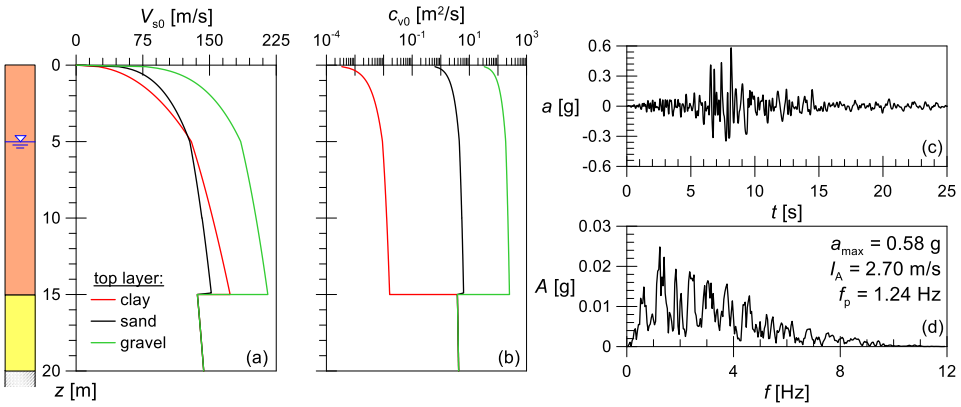

Fig. 1. Profiles of initial shear waves velocities (a) and initial consolidation coefficients (b) in the soil column, (c) input signal, and (d) Fourier Amplitude spectra of the Northridge (1994) earthquake (a_{max} = maximum acceleration; I_A = Arias Intensity; f_p = dominant frequency).

3.1 Calibration of model parameters for the decoupled approach

To have a consistent comparison between the results of the fully *coupled* FEM analyses and those provided by the *decoupled* FDM method, model parameters required for the simplified approach were calibrated using a series of undrained and drained numerical cyclic shear tests carried out with the *Plaxis Soil Test* tool.

As for the r_u-r_N (Eq. (4)) and the *CSR*-N_L (Eq. (5)) curves, undrained cyclic shear tests were simulated with a static vertical effective stress σ'_{v0} = 220 kPa, representative of the effective stress state at the centre of the liquefiable layer. The excess pore pressure equation r_u-r_N was calibrated applying *CSR* values in the range 0.25 - 0.05, and the cyclic resistance curve *CSR*-N_L was obtained considering the triggering of liquefaction

at r_u = 0.9. Fig 2 shows the two curves obtained with the best-fitting values of the coefficients χ and θ (Fig. 2a), and CSR_t, β and η (Fig. 2b).

Table 2. *HSSmall* model parameters assumed for the non-liquefiable layer

Soil	G_0^{ref} (MPa)	m (-)	$\gamma_{0.7}$ (-)	E_{ur}^{ref} (MPa)	ν_{ur} (-)	$E_{ur}^{ref}/E_{50}^{ref}$ (-)	$E_{50}^{ref}/E_{oed}^{ref}$ (-)	R_f (-)
clay	51.8	0.84	$1.0 \cdot 10^{-3}$	46.1	0.2	3.0	1.0	0.9
sand	47.1	0.50	$2.4 \cdot 10^{-4}$	56.5	0.2	3.0	1.0	0.9
gravel	94.7	0.44	$2.4 \cdot 10^{-4}$	113.6	0.2	3.0	1.0	0.9

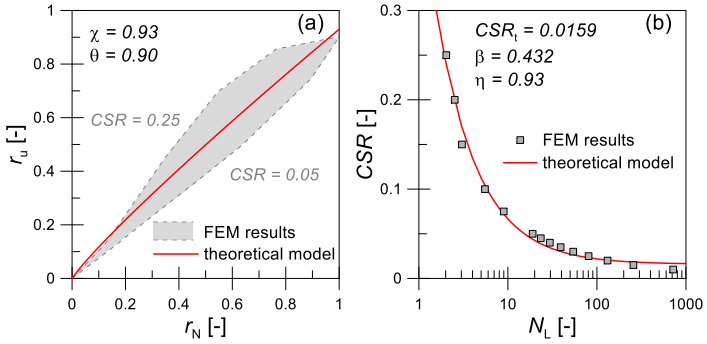

Fig. 2. (a) Excess pore pressure ratio and (b) cyclic resistance curves adopted in the *decoupled* approach.

The 1D SRAs were carried out using the nonlinear soil model proposed by Conti *et al.* [10], which is defined by six parameters: the shear strength, τ_{lim}, and the small-strain shear modulus, G_0; *a* and *b*, defining the shear modulus decay curve; and *c* and *d*, defining the hysteretic damping curve. Parameters *a*, *b*, *c*, and *d* were calibrated based on the results of numerical drained cyclic shear tests, carried out at a static vertical effective stress σ'_{v0} = 150 kPa, applying a 10 cycles/s sinusoidal shear strain time history. The resulting shear modulus decay and damping curves are plotted in Fig. 3, together with those adopted in the nonlinear total stress SRAs.

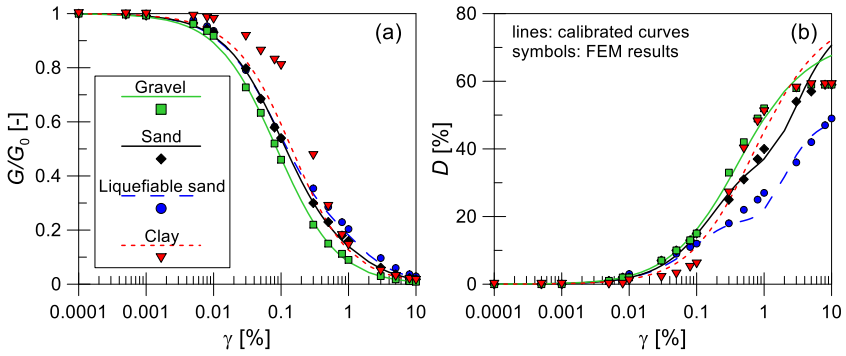

Fig. 3. (a) Shear modulus decay and (b) damping curves adopted in the total stress SRAs (line), calibrated against FEM simulations (symbols).

3.2 Results

Fig. 4 compares the space-time contours of the excess pore pressure ratio r_u obtained with the *coupled* (FE) and the *decoupled* (FD) approach. In all cases, complete liquefaction occurs at the bottom of the soil column, due to the high intensity of the seismic event and the distance from the drainage boundary. Conversely, at the interface between the two layers, the development of excess pore water pressures is strongly influenced by the hydraulic condition imposed by the top, non-liquefiable, soil. In the first configuration, the presence of a highly-permeable gravelly layer inhibits the occurrence of complete liquefaction at the top of the underlying sand. In the second configuration, the excess pore water pressures generated in the liquefiable sand spread out through the upper sandy layer. As a result, the diffusion process causes a reduction in strength and stiffness also in the upper layer during the early stages of the applied earthquake. Finally, when the upper layer consists of a low-permeability clayey soil (third configuration), the deepest layer completely liquefies and, as expected, a negligible redistribution of excess pore water pressure takes place in the top soil. Furthermore, Fig. 5 shows the time histories of the excess pore pressure ratio r_u in the middle of the liquefiable sand layer, obtained with FD and FE analyses. The time interval was extended to 75 s, to compare the purely dissipative phase following the seismic event. The importance of the hydraulic conductivity of the top layer is also highlighted in this figure, which shows a decreasing dissipation rate going from the case with a gravelly layer to the one with clayey crust. The *decoupled* approach provides slightly faster dissipation processes than the FE analyses but, despite its simplicity, the results are in a good agreement with the FE ones.

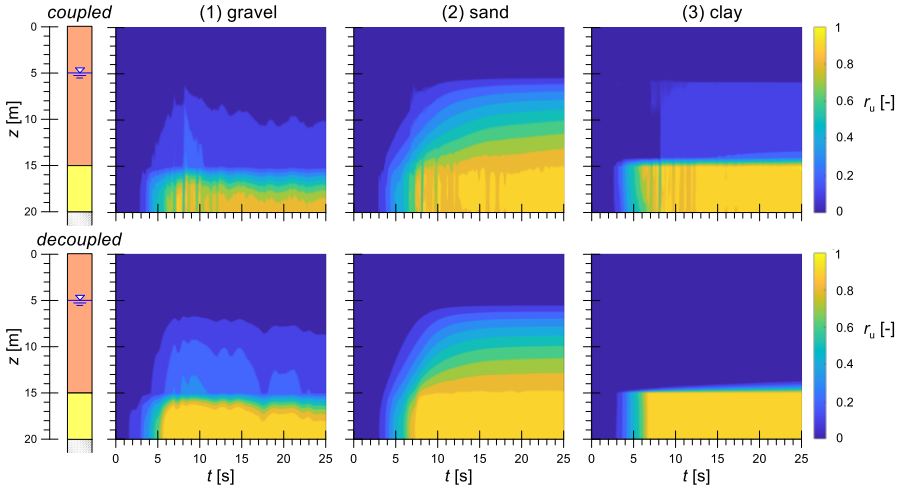

Fig. 4. Comparison of contours of r_u obtained with the *coupled* and *decoupled* analyses.

4 Conclusions

In this paper, a *decoupled* approach was presented to provide a tool for assessing the liquefaction hazard of sandy soils, based on the work by Seed *et al.* [1]. An equivalent natural frequency of the soil column was introduced, depending on the excess pore water pressures, so as to consider the shift in frequency content of the propagated signal due to the soil stiffness degradation. Moreover, the assumption of uniform time distribution of the number of equivalent cycles was replaced with a more realistic energy hypothesis. The proposed approach, implemented in a *Matlab* routine through the FDM, was validated against the results of *fully-coupled* dynamic FE analyses. The results of FDM and FE analyses turned out to be in a very good agreement, providing confidence in the predictive capability of the proposed simplified approach.

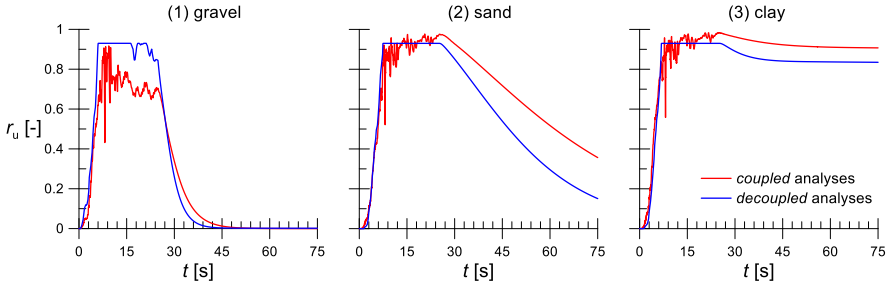

Fig. 5. Comparison of time histories of r_u in the middle of the liquefiable layer (z = 17.50 m) obtained with the *coupled* and *decoupled* analyses. The time interval was considered three times that of the seismic event duration.

References

1. Seed, H.B., Martin, P.P., Lysmer, J.: The generation and dissipation of pore water pressures during soil liquefaction. College of Engineering, University of California (1975)
2. Dafalias, Y.F., Manzari, M.T.: Simple plasticity sand model accounting for fabric change effects. J Eng Mech 130(6), 622-634 (2004).
3. Boccieri G., Gaudio D., Conti R: A simplified method for the estimation of earthquake-induced pore pressure. Geotechnical Engineering for the Preservation of Monuments and Historic Sites III. CRC Press, 812-822. DOI: 10.1201/9781003308867-62. (2022).
4. Mathworks Inc. Matlab version 9.10.0 (R2021a). Natick, Massachusetts (2021).
5. Bentley. Plaxis 2D CE v20 – Reference Manual. Delft University of Technology. Delft, The Netherlands. (2020).
6. Terzaghi, K.: Die Berechnung der Durchassigkeitsziffer des Tones aus dem Verlauf der hydrodynamischen Spannungs. erscheinungen. Sitzungsber. Akad. Wiss. Math. Naturwiss. Kl. Abt. 2A 132: 105-124. (1923).
7. Wichtmann, T., Triantafyllidis, T.: Effect of uniformity coefficient on G/Gmax and damping ratio of uniform to well-graded quartz sands. J Geotech Geoenv Eng, 139(1), 59-72 (2013).
8. Hancock, J. Bommer, J.J.: The effective number of cycles of earthquake ground motion. Earthq Eng Struct Dyn 34(6): 637-664 (2005).
9. Benz, T.: Small-strain stiffness of soils and its numerical consequences. Ph.D. thesis, University of Stuttgart (2006).
10. Conti, R., Angelini, M., Licata, V.: Nonlinearity and strength in 1D site response analyses: A simple constitutive approach. Bull Earthq Eng 18: 4629-4657 (2020).